Biophysical Chemistry, 38 (1990) 143–154
Elsevier

BIOCHE 01508

The interaction of bile salt micelles with the dansyltyrosine derivatives of porcine colipase

Jonathan C. McIntyre [a], Friedhelm Schroeder [b,c] and W. David Behnke [a]

[a] *Department of Molecular Genetics, Biochemistry and Microbiology, College of Medicine,*
[b] *Department of Pharmacy and Medicinal Chemistry, College of Medicine and* [c] *Department of Pharmacology and Cell Biophysics, College of Pharmacy, University of Cincinnati, Cincinnati, OH 45267, U.S.A.*

Received 1 October 1989
Revised manuscript received 24 January 1990
Accepted 17 May 1990

Colipase; Interface recognition site; Time-resolved fluorescence; Dansylaminotyrosine; Micelle binding

The interaction of bile salt micelles with the tyrosines of pancreatic colipase was assessed by steady-state and time-resolved fluorescence techniques. Dansyltyrosine fluorescence showed that Tyr-55 was located in the proposed interface recognition site. In support of this claim was a 70 nm blue shift and 4.3-fold quantum yield increase in emission spectrum due to taurodeoxycholate (TDOC) micelle-complex formation. Complex formation also caused a shift in the center of the major lifetime distribution from 11.7 to 15.1 ns, and more than doubled the polarization and anisotropy decay parameters. These data supported an earlier model of colipase-micelle binding that suggested that Tyr-55 was inserted into the interior of the TDOC micelle upon binding (J.C. McIntyre, P. Hundley and W.D. Behnke, Biochem. J. 245 (1987) 821). Identical experiments on a DNS-Tyr-59 derivative of colipase showed that Tyr-59 did not specifically interact with micelles. Moreover, acrylamide quenching data suggest an alteration in the protein environment surrounding DNS-Tyr-59 such that during complex formation, the efficiency of quenching of DNS-Tyr-59 increases.

1. Introduction

For many years chemical modification has been a powerful tool of protein chemists and enzymologists for the study of protein structure-function relationships. Residues located in the active site of an enzyme may be tentatively identified by the use of chemical modification [1]. The incorporation of a spectroscopic probe can monitor conformational transitions in a protein [2,3]. Recently, the use of site-directed mutagenesis has refined the way in which the chemical constituents of a protein can be altered [4]. Nevertheless, chemical modification is still useful for identifying areas in a protein that are important for function. In fact, the combination of chemical modification for targeting important residues and site-directed mutagenesis for detailed functional studies is a strategy that has been used in many systems [5a,5b]. A previous article describes the synthesis and characterization of *o*-aminodansyl derivatives of the tyrosine residues in porcine pancreatic colipase [6]. These modifications were designed so as to assess the role of tyrosine residues in the lipid recognition

Correspondence address: W.D. Behnke, Department of Molecular Genetics, Biochemistry and Microbiology, College of Medicine, University of Cincinnati, Cincinnati, OH 45267, U.S.A.

Abbreviations: 2D, two dimensional; CMC, critical micellar concentration; TDOC, taurodeoxycholate; NEM, *N*-ethylmaleimide; photo-CIDNP, photochemically induced dynamic nuclear polarization; PLA2, phospholipase A_2; dansyl (DNS), 5-(dimethylamino)-1-naphthalenesulfonyl; DNS-Tyr-55, DNS-Tyr-59 and DNS-Gly-1 porcine colipases, *o*-aminodansyltyrosine 55, *o*-aminodansyltyrosine 59 and *o*-aminodansylglycine 1 (N-terminal) derivatives of porcine colipase, respectively.

0301-4622/90/$03.50 © 1990 Elsevier Science Publishers B.V. (Biomedical Division)

site of colipase. Herein is presented a spectrofluorometric analysis of the interaction of bile salt micelles (a model for bile salt coated fat emulsions) with these fluorescently labelled proteins.

It has recently been established that Tyr-55 is located on the surface of the molecule where it rotates freely [6]. Emission spectrum, lifetime analysis, acrylamide quenching, static polarization and anisotropy decay experiments all verify this conclusion [6]. Other studies using techniques such as NMR, CD, ultraviolet difference spectroscopy and photo-CIDNP [7–10] are in agreement with fluorescence investigations indicating that one of the three tyrosines of colipase is located on the surface of the protein. However, the surface tyrosine identified by NMR was either Tyr-58 or Tyr-59 [7]. The NMR studies also suggested that one of the three tyrosines residues is thoroughly buried in the protein interior and another is in a partially buried position in the molecule. The buried tyrosyl residue according to NMR data was Tyr-55. These resonance assignments were based on pH titration and decoupling experiments, and no rationale was given for assigning the buried tyrosyl residue to position 55. Chemical modification and spectrofluorometric studies of the dansyl modified colipases — specifically; quenching, anisotropy decay and polarization experiments — have identified the partially buried tyrosine at position 59 [6]. The identification and establishment of the environments of the three tyrosines have been reassessed by chemical modification and fluorescence spectroscopy, and suggest that the earlier NMR experiments should be repeated to include sequence-specific assignments based on COSY and NOESY experiments. Thus, the role of these tyrosyl residues, numbers 55 and 59, in the proposed interface recognition site will be examined with the same probes.

Comparison of the preliminary steady-state fluorescence studies of DNS-Tyr-55 porcine colipase [11] with similar investigation of the tyrosines of phospholipase A_2 shows remarkable similarities [12]. Aminodansylation of Tyr-19 of equine PLA2 improves the affinity of the enzyme for lipid-water interfaces. The binding of the aminodansylated PLA2 to an oil/water interface causes a 27 nm blue shift and 400% quantum yield increase in the fluorescence spectrum. It was concluded that the increased binding and dramatic fluorescence changes were the result of the insertion of the dansyltyrosine group into the interior of the lipid interface. Recent X-ray crystallographic analysis of bovine phospholipase A_2 implicates Ile-19 (this is a tyrosine in the equine system) as being oriented in space in such a manner to make this residue part of the interface recognition site [13a,b]. Isoleucine would interact in a hydrophobic capacity in such an environment. The activity of the dansyltyrosine-55-modified protein is actually double that of the native enzyme [11]. It also shows a characteristic hydrophobic blue shift and quantum yield increase in fluorescence emission in the presence of TDOC micelles [11]. The addition of a hydrophobic group at the proposed lipid recognition site of the colipase molecule might increase its affinity for lipid interfaces, therefore increasing the amount of actively adsorbed lipase. In view of the striking similarities in the steady-state fluorescence experiments between dansylaminotyrosine derivatives of phospholipase A_2 and colipase, insertion of Tyr-55 into the micelle interior may be part of the binding mechanism of colipase to interfaces.

To study more thoroughly the possibility that tyrosine insertion is a mechanism of micelle binding; lifetime analysis, polarization, anisotropy decay and acrylamide quenching studies are presented here, in an attempt to validate earlier steady-state investigations. Binding parameters from these experiments are also presented and support the possibility that the nature of the increased activity of DNS-Tyr-55 porcine colipase is related to an increased affinity of the modified protein for interfaces. These studies are extended to dansyl-modified Tyr-59 so as to determine the role of Tyr-59 in the lipid recognition site.

2. Materials and methods

2.1. Proteins and reagents

Porcine pancreatic lipase was kindly provided by M. Rovery and colleagues from the Centre de Biochimie et de Biologie Moleculaire du Centre

National de la Recherche Scientifique, Marseilles, France. Porcine colipase was isolated according to the procedure of Chapus et al. [14]. Acetone powders of porcine pancreas were generated from fresh tissue (Kahns Meats, Cincinnati, OH) in our laboratory. Dimethylmaleic anhydride and TDOC were purchased from Sigma (St. Louis, MO.). TLC analysis of several different commercial TDOC samples showed significant fluorescent contamination. Lot numbers without such contamination were used for all fluorescence measurements, with solution preparation taking place the same day as use. Micropolyamide sheets for 2D TLC of dansylated amino acids were purchased from Pierce (Rockford, IL). All other chemicals were obtained as described in ref. 6. Dansyltyrosine derivatives of colipase were synthesized and characterized as described earlier [6].

2.2. Synthesis and characterization of N-terminal dansyl-porcine colipase

To 10 mg of porcine pancreatic colipase in 1.0 M sodium bicarbonate (pH 9.0, 4°C) was added 40 mg of dimethylmaleic anhydride in 10-mg aliquots. The pH of the reaction was kept at 9.0 by the addition of 6 N HCl and the reaction was allowed to proceed for 60 min. The reaction generated a modified form of colipase with all four lysine groups being reversibly acylated [15]. The reaction products were extensively dialyzed against 0.1 M bicarbonate buffer (pH 6.9). The dialysate was then reacted with a 10-fold molar excess of dansyl chloride at room temperature in the dark for 24 h. The acylated lysines were deblocked by extensive dialysis against pH 6.0 buffer [15]. The final product had an absorbance spectrum with a maximum at 350 nm. By the combined use of a Lowry protein assay and the absorbance at 350 nm ($E_{m\ 350\ nm} = 3980\ M^{-1}\ cm^{-1}$) [16], it was shown that the modified protein contained 0.91 mol dansyl/mol colipase. The enzyme activity of the modified protein was 80% of that of the native protein. N-terminal analysis by acid hydrolysis and 2D TLC (1st dimension, benzene/water, 9 : 1; 2nd dimension, water/formic acid, 100 : 1) showed the presence of *N*-dansylglycine, glycine being the N-terminal amino acid of porcine colipase AII. Emission spectra and lifetime analysis showed no significant changes with increasing TDOC concentrations (data not shown).

2.3. Instrumentation

Ultraviolet and visible absorbance measurements were made on a Cary 15 scanning spectrophotometer (Varian, Monrovia, CA). Static fluorescence measurements were taken on a Perkin-Elmer MPF-44A equipped with a DCSU-2 corrected spectra unit (Norwalk, CT). Time-resolved fluorescence and differential polarization experiments were performed on an SLM 4800 subnanosecond spectrofluorometer modified to a 1–250 MHz multifrequency capacity [17–20]. A Liconix He/Cd laser was used as the light source with an emission line at 325 nm that was sinusoidally modulated with a Pockels cell. The modulated emission was observed in the L-format through a Janos GG-375 cut-off filter for both lifetime and differential polarization measurements. The data were collected by an IBM-PC with ISS-01 and ISS-187 software (ISS Instruments, Urbana, IL).

2.4. Lifetime and differential polarization measurements

The acquisition of both lifetime and differential polarization data was performed as described previously [6,17–20]. Phase and modulation data were collected at 8–16 modulation frequencies (15–170 MHz) with respect to the reference fluorophore dimethyl-POPOP in absolute ethanol (lifetime 1.45 ns) [21]. The excitation polarizer was set at the magic angle, 55°, in order to eliminate Brownian motion as a determinant of apparent lifetime. Data were collected and analyzed by ISS-1 and ISS-187 software. Lifetime analysis was performed by either a nonlinear least-squares analysis [22], or a Lorentzian continuous distribution analysis [23,24] for a one-, two- or three-component fit. Lorentzian continuous distribution analysis was favored for this work due to the added dimension of measuring width distributions. The ability to measure width distributions provides additional evidence for the homogeneity of a particular emitting species, which can be very informative in

protein studies [25,26]. The reduced χ^2 parameter was used to judge quality of fit [6].

Differential phase and modulation ratio experiments were carried out in order to obtain static polarization values. These values and previously reported lifetime data were used to calculate time-resolved anisotropies [17–19]. Data were collected by ISS-01 software utilizing the differential polarization program and calculated by the rotational least-square analysis program, which fits the data to eq. 1:

$$F(t) = \sum_j [1 + a \cdot r(t)] \cdot i(t) \quad (1)$$

where the following eqs 2 and 3 represent $r(t)$ and $i(t)$, respectively:

$$r(t) = \sum_l [1 + a \cdot g_l \cdot \exp(-t/R_l)] \quad (2)$$

$$i(t) = \sum_i [f_i \cdot \exp(-t/T_i)] \quad (3)$$

The following indices represent constants that depend upon the nature of the sample being observed; j is the number of species present, l indicates the number of rotational components for each species, and i represents the number of lifetime components for each species. T_i and f_i are the values of emission lifetime and fractional intensity, respectively. The summation of the fractional contributions g_1 is the limiting anisotropy. The rotational correlation times are represented by R_l.

From this, it is possible to calculate anisotropy decay parameters from one set of data in several different ways. However, only the hindered rotator model was used to calculate anisotropy decay data (eq. 4):

$$r(t) = (r_0 - r_{inf}) \exp(-t/R) + r_{inf} \quad (4)$$

In eq. 4 r_{inf} represents the limiting anisotropy at infinite time. The number of possible rotational components of a complex system involving the binding of one large molecule to a large aggregate was beyond our resolution. In a system such as this, the correlation times of the unbound protein, the complex and the segmental motion of the fluorophore are all very similar and therefore difficult to resolve individually. Fitting the data to eq. 4 results in rotational relaxation times and limiting anisotropies which are complex averages that cannot be interpreted literally. The determination of the quantities is, however, useful for detecting changes and differences among the colipases and serves as a basis for comparison. Protein concentration in both lifetime and differential polarization studies was chosen to be below a value of 0.20 absorbance units at 325 nm, so as to eliminate inner filter effects. The concentration of TDOC used in these experiments was chosen to start below CMC and to approach binding saturation.

2.5. Acrylamide quenching

Acrylamide quenching experiments were performed by monitoring the change in the fluorescence emission spectra induced by the addition of acrylamide. A solution of 8 M acrylamide was used, and to determine the extent of the dilution factor identical experiments were performed using distilled water. The emission spectra were obtained in the corrected mode with an excitation wavelength of 335 nm. The data are presented as K_{sv} values according to eq. 5 [27]:

$$F_0/F \exp(V[Q]) = 1 + K_{sv}[Q] = F^\circ/F \quad (5)$$

K_{sv} values are obtained by measuring the slope of the line generated by plotting F°/F vs [Q].

3. Results

As described in our previous articles [6,11], the use of dansyltyrosine derivatives of colipase was established to generate sensitive probes of protein microenvironments. These studies were designed to determine the role of tyrosine residues in the lipid recognition site of pancreatic colipase. In addition to the static emission spectra of the original investigation [11], lifetime, polarization and anisotropy decay experiments were utilized in this study. These measurements allowed for the determination of the dynamic interaction of the fluorophores with TDOC micelles.

3.1. The effect of TDOC on the emission spectra of DNS-Tyr-55 porcine colipase and DNS-Tyr-59 porcine colipase

The emission spectra of DNS-Tyr-55 porcine colipase and DNS-Tyr-59 porcine colipase are shown in fig. 1A and B, respectively. The addition of 4.0 mM TDOC caused the emission spectrum of DNS-Tyr-55 porcine colipase to shift from 550 to 480 nm, a 70 nm blue shift. This shift in emission maximum was accompanied by a 4.3-fold quantum yield increase. The effect of TDOC on the emission spectrum of DNS-Tyr-59 porcine colipase was not nearly as dramatic as the changes in the Tyr-55-modified colipase. In the presence of TDOC micelles, the emission maximum of 520 nm did not change, and the quantum yield increased only 2.5-fold.

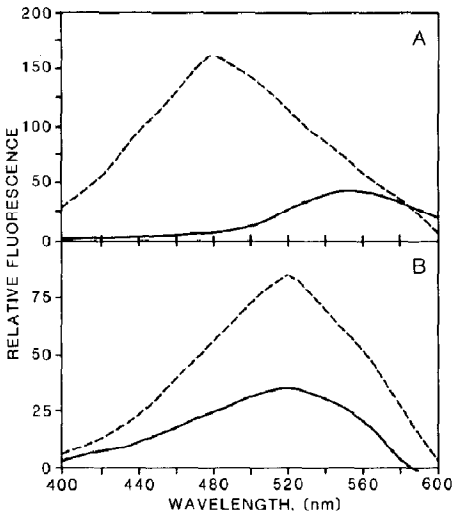

Fig. 1. Effect of bile salt micelles on the emission spectra of DNS-Tyr-55 porcine colipase and DNS-Tyr-59 porcine colipase. Spectra were obtained in the corrected mode with an excitation wavelength of 325 nm and 8 nm slit widths for both excitation and emission. The proteins were dissolved into a 0.05 M K_2HPO_4 (pH 7.4) buffered solution. A taurodeoxycholate stock solution (0.10 M) was made with the same buffer and all spectra were obtained at room temperature. The plots depicted in panel A have been reported previously [6,11]. (A) (———) 0.56 mg/ml DNS-Tyr-55 porcine colipase, (- - - - -) 0.56 mg/ml DNS-Tyr-55 porcine colipase with 4 mM TDOC. (B) (———) 0.56 mg/ml DNS-Tyr-59 porcine colipase, (- - - - -) 0.56 mg/ml DNS-Tyr-59 porcine colipase with 4 mM TDOC.

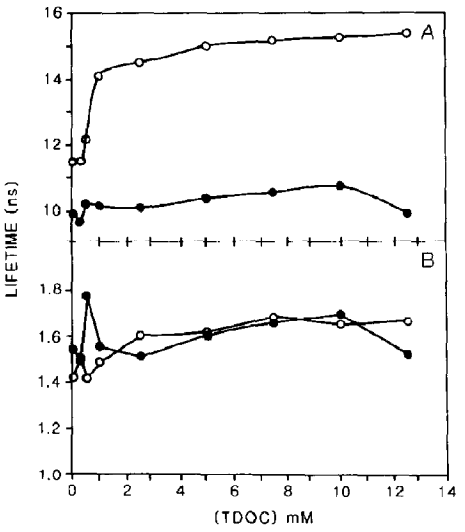

Fig. 2. Effect of TDOC concentration on the center of the lifetime distribution of DNS-Tyr-55 porcine colipase and DNS-Tyr-59 porcine colipase. All measurements were made at 24°C with a 325 nm excitation wavelength. The buffered solution was 0.05 M K_2HPO_4 (pH 7.4) and the stock TDOC solution was made in the same buffer. (A) Center of the major lifetime distribution (in ns): (○———○) 30.6 μg/ml DNS-Tyr-55 porcine colipase and (●———●) 32.0 μg/ml DNS-Tyr-59 porcine colipase. (B) Center of the minor lifetime distribution (in ns): (○———○) 30.6 μg/ml DNS-Tyr-55 porcine colipase and (●———●) 32.0 μg/ml DNS-Tyr-59 porcine colipase.

3.2. Lifetime distribution analysis

The lifetimes of Tyr-55- and Tyr-59-modified porcine colipase were determined by Lorentzian continuous distribution and nonlinear least squares analyses. Only the distribution analyses are presented here, with $C[1]$ representing the center of the width of the major lifetime distribution and $C[2]$ denoting the same relationship for the minor distribution. The advantages of using the Lorentzian method were discussed previously [6]. The effect of increasing TDOC concentration on both lifetime components is presented in fig. 2. The center of the first lifetime distribution of DNS-Tyr-55 porcine colipase (fig. 2A) showed

very minor changes until the CMC of TDOC was reached at 1.0 mM. At the CMC, the lifetime increases 22% from 11.5 to 14.1 ns. This increase gradually saturated at higher concentrations of TDOC, reaching 15.4 ns at 12.5 mM TDOC which was the same as the lifetime of the model compound *N*-acetyl-3-dansyltyrosine ethyl ester in the viscous solvent propylene glycol. A shift to longer lifetimes is indicative of a more hydrophobic environment for the fluorophore, and would support earlier conclusions made from the emission spectra data for DNS-Tyr-55 porcine colipase. The center of the minor lifetime distribution component of DNS-Tyr-55 porcine colipase was not affected by increasing TDOC concentrations, nor is the second component of DNS-Tyr-59 porcine colipase. This result may be due to rotational isomers of dansylaminotyrosine which have geometries that do not allow the fluorophore to interact with micelles. The $C[1]$ of DNS-Tyr-59 porcine colipase showed a very marginal increase with increasing TDOC, and stayed near 10 ns. Thus, the lifetime distribution of DNS-Tyr-59 porcine colipase was insensitive to TDOC binding, in contrast to the quantum yield increase seen in the emission spectra.

3.3. Acrylamide quenching of dansyl-modified colipases with and without TDOC micelles

Fluorescence intensity was used to monitor the quenching of dansyl fluorescence by acrylamide. To explore the change in dansyltyrosine environment when the protein is bound to TDOC micelles, Stern-Volmer constants from acrylamide quenching of dansyl colipases and dansyl colipases complexed with micelles were determined (table 1). The Stern-Volmer constant (K_{sv}) for DNS-Tyr-55 porcine colipase was significantly greater than that of DNS-Tyr-59 porcine colipase, indicating that Tyr-55 was much more accessible to the surface than Tyr-59. When bound to micelles, the quenching of DNS-Tyr-55 was reduced by 64%. The shielding from quenchers provided by TDOC suggests that Tyr-55 is located in the lipid recognition site and may insert into the interior of the micelle as part of the mechanism of binding. The Stern-Volmer constants for DNS-Tyr-59 porcine colipase with 10.0 mM TDOC increased instead of decreased. The K_{sv} increased almost 3-fold. These data indicate that Tyr-59 actually becomes more accessible to quenching when the protein is bound to micelles.

Table 1

Acrylamide quenching of DNS-Tyr-55 porcine colipase and DNS-Tyr-59 porcine colipase

Stern-Volmer quenching constants (K_{sv}) were calculated for acrylamide quenching of DNS-Tyr-55 porcine colipase and DNS-Tyr-59 porcine colipase. $K_{sv}(F)$ represents the Stern-Volmer constant for acrylamide quenching of the steady-state emission and is calculated from a plot of F_0/F vs [acrylamide].

Sample	$K_{sv}(F)$ (M^{-1})
DNS-Tyr-55 porcine colipase	5.83
+10 mM TDOC	2.11
DNS-Tyr-59 porcine colipase	0.79
+10 mM TDOC	2.33

3.4. Static polarization studies of colipase-micelle binding

The N-terminal dansyl derivative of colipase was synthesized in an attempt to attach covalently a dansyl group to colipase in a region of the molecule that did not directly interact with bound micelle. This type of probe could be used to ascertain the effect of the increased size of the colipase-micelle complex on the static polarization of the protein, and by inference would allow for the determination of local effects at Tyr-55 and Tyr-59. However, the values generated by these measurements (P, R, and r_∞) are complicated and depend upon protein tumbling, segmental motion and the location of the fluorophore's transition moment with respect to the major axis of the protein and the complex. Thus, these numbers are used for comparison, and only large differences can be regarded as significant. DNS-Gly-1 porcine colipase was unaffected by TDOC micelle binding as observed by steady-state emission spectral and lifetime analyses, and thus was used as a control in static polarization and anisotropy decay experiments.

The polarization of DNS-Gly-1 porcine colipase increased gradually from 0.119 at 1.0 mM TDOC to 0.136 at 12.5 mM TDOC (fig. 3). The

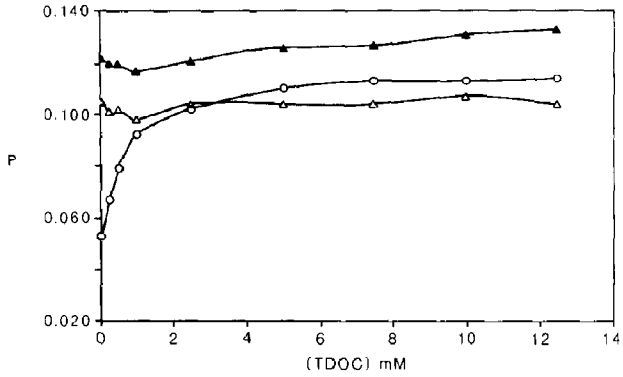

Fig. 3. Effect of TDOC concentration on the polarization of dansyl derivatives of colipase. All measurements were made at 24° C in 0.05 M K_2HPO_4 (pH 7.4) buffer. The instrument was set for L-format measurements. (○———○) 30.6 μg/ml DNS-Tyr-55 porcine colipase, (△———△) DNS-Tyr-59 porcine colipase and (▲———▲) 36.5 μg/ml DNS-Gly-1 porcine colipase.

14% increase in polarization can be attributed to the slower rotational correlation time of the colipase-micelle complex, and was used as the standard increase in polarization due to complex formation. The polarization value of DNS-Tyr-55 porcine colipase increased 100% from 0.055 at 0 mM TDOC to 0.110 at 12.5 mM TDOC. In comparison to DNS-Gly-1 porcine colipase, this polarization increase indicated that the rotation of the dansyl group at Tyr-55 had been restricted due to steric hindrance and/or viscosity changes. Steric hindrance at Tyr-55 could arise from a direct interaction with the interior of the micelle or from the protein itself. For the protein interior to be the cause of the change in environment for Tyr-55, the protein would have to undergo a radical conformational change that has not been observed in other physical studies. The polarization data supported emission spectra, lifetime, and quenching experiments, all of which indicated a dramatic change in the environment of Tyr-55 consistent with its burial in a hydrophobic region when colipase is bound to micelles. The polarization of DNS-Tyr-59 porcine colipase does not change over the range of TDOC concentration used suggesting that DNS-Tyr-59 is not hindered by complex formation.

3.5. *Anisotropy decay calculations*

Anisotropy decay data were calculated from lifetime and differential polarization data using the hindered rotator model to resolve an averaged rotational relaxation time (R) (fig. 4) and limiting anisotropy (r_{inf}) (fig. 5). Comparison of the ani-

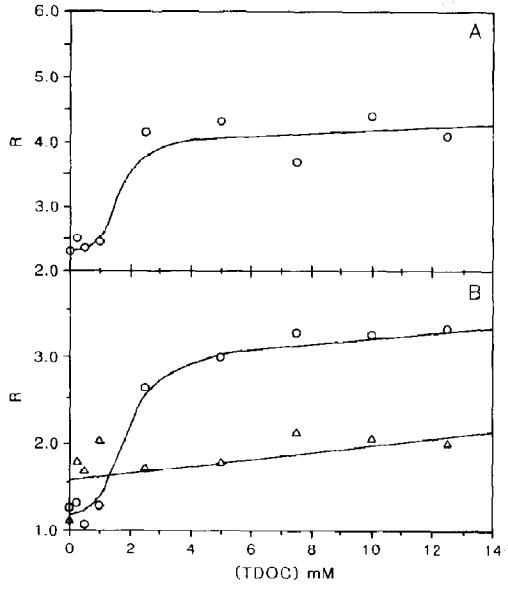

Fig. 4. Rotational relaxation time calculations for varied taurodeoxycholate concentrations. R, the rotational correlation time (in ns), was obtained from anisotropy decay calculations utilizing the hindered rotator model. The input for data for anisotropy decay calculations was the lifetime and differential polarization parameters from experiments outlined in figs 2 and 3. (A) (○———○) DNS-Gly-1 porcine colipase; (B) (○———○) DNS-Tyr-55 porcine colipase and (△———△) DNS-Tyr-59 porcine colipase.

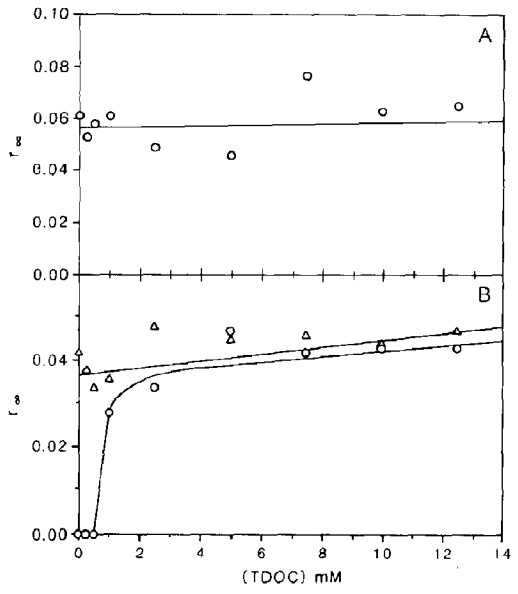

Fig. 5. Limiting anisotropy calculations for varied TDOC concentration. The r (r_{inf}) [limiting anisotropy at times much greater than emission] was obtained from anisotropy decay calculations utilizing the hindered rotator model. The input for calculations was the lifetime and differential polarization parameters from experiments outlined in figs 2 and 3. (A) (○——○) DNS-Gly-1 porcine colipase; (B) (○——○) DNS-Tyr-55 porcine colipase and (△——△) DNS-Tyr-59 porcine colipase.

sotropy decay parameters of DNS-Tyr-55 porcine colipase and DNS-Tyr-59 porcine colipase vs DNS-Gly-1 porcine colipase allows for the determination of local rotational dynamic effects, when the protein is bound to TDOC micelle. The rotational relaxation time of DNS-Gly-1 porcine colipase increased from 2.3 ns, in the absence of TDOC, to 4.3 ns at 12.5 mM TDOC. This 87% increase in R was due to slower tumbling of the micelle-colipase complex. Small-angle neutron scattering and analytical ultracentrifugation data have shown that the average micelle contains 20–22 monomers of TDOC and that these micelles are ellipsoidal with an approximate molecular weight of 10000 [28,29]. Therefore, the doubling of molecular weight that accompanies complex formation generated a considerable (87%) increase in rotational relaxation rate. Titration of DNS-Tyr-55 porcine colipase with TDOC caused a 191% increase in R. By comparison to DNS-Gly-1 porcine colipase, these data suggest that the binding of micelle to colipase alters the local rotational properties of dansyl-Tyr-55 in a manner that slows the rotation of the fluorophore. The R value of DNS-Tyr-59 porcine colipase increased only 67% over the same range of TDOC concentration.

The anisotropy decay parameter r_{inf} is a measure of the degree to which the rotation of a fluorophore is hindered. A zero or negative value of r_{inf} indicates that the rotational path is free from hindrance, while larger positive values of r_{inf} correspond to a greater energy barrier to all angles of displacement [30]. The r_{inf} value of DNS-Gly-1 porcine colipase did not change when bound to micelle. The r_{inf} value of DNS-Tyr-55 porcine colipase in the absence of TDOC showed that Tyr-55 was free to rotate through all possible angles of displacement. This was maintained until 1.0 mM TDOC where r_{inf} became positive. This is, therefore, indicative of a hindered rotation for DNS-Tyr-55 when colipase is bound to TDOC micelle. Only a very slight increase r_{inf} was observed when DNS-Tyr-59 porcine colipase was titrated with TDOC micelles.

Table 2 summarizes the effects of bile salt micelle binding on the polarization and anisotropy decay of all three modified colipases. Table 2 clearly shows by comparison that the observed changes in the rotational parameters of DNS-Tyr-55 porcine colipase far exceeded those in the other two reference colipases. By the same type of comparison, it was shown that DNS-Tyr-59 is not hindered when colipase is bound to a micelle.

Table 2

Percent increase in polarization and anisotropy decay parameters due to micelle binding

Percent increases were calculated from the graphs in figs 3–5. P, polarization (from fig. 3); R, rotational relaxation time (from fig. 4); r_{inf} (r_∞), limiting anisotropy (from fig. 5).

Sample	Increase (%)		
	P	R	r_{inf}
DNS-Gly-1 porcine colipase	14	83	0–3
DNS-Tyr-55 porcine colipase	100	191	400
DNS-Tyr-59 porcine colipase	0–2	67	2–7

Table 3

Scatchard analysis of TDOC micelle binding to DNS-Tyr-55 porcine colipase

Dissociation constants (K_d) were determined by Scatchard analysis of the titration of DNS-Tyr-55 porcine colipase with TDOC. Binding was monitored by the change in the physical parameters: C[1], center of the major lifetime component (from fig. 2); P, polarization (fig. 3); R, rotational relaxation time (fig. 4); r_{inf} (r_∞), limiting anisotropy (fig. 5).

	C[1]	P	R	r_{inf}
DNS-Tyr-55 porcine colipase	5.3×10^{-5} M	1.5×10^{-5} M	8.0×10^{-6} M	3.8×10^{-5} M

3.6. Scatchard analysis of the binding of bile salt micelles to DNS-Tyr-55 porcine colipase

Dissociation constants for the binding of micelles to DNS-Tyr-55 porcine colipase shown in table 3 were determined by Scatchard analysis [31]. Saturation binding concentration was determined by a double-reciprocal plot of 1/(physical parameter in question) vs 1/micelle (20 monomers of colipase per micelle; CMC = 1.0 mM). All Scatchard plots were linear, showing no cooperative binding and the x-intercept indicated a single binding site, in agreement with earlier studies [9,28]. The previous studies determined a K_d of 10^{-4} M for TDOC micelle-colipase binding [9,28]. Binding parameters were calculated by monitoring four different fluorescence parameters in an attempt to determine whether aminodansylation of Tyr-55 increases the affinity of colipase for micelles. An increased affinity for lipid interfaces may explain the greater activity of DNS-Tyr-55 porcine colipase. All four of the sets of data (C[1], P, R, r_{inf}) showed that DNS-Tyr-55 porcine colipase has an increased affinity for bile salt micelles compared to unmodified colipase [9,28]. The binding affinities ranged from 2- to 12.5-times greater than that of the native protein [9,28] with an average of 6-times greater affinity for TDOC micelles.

4. Discussion

The mechanisms by which water-soluble enzymes and proteins recognize and adsorb to lipid interfaces have long been under investigation in many different systems [32]. Studies on the binding of colipase to model lipid interfaces have centered around the use of physical methods to determine structural changes in colipase as a result of binding. In keeping with the spirit of these previous efforts, herein is presented chemical modification and spectrofluorometric studies of the tyrosine residues in the proposed interface recognition site of porcine pancreatic colipase. A previous work reported the synthesis of two specific modified forms of colipase [6], aminodansylated at Tyr-55 or Tyr-59. These modified colipases were generated to provide unique probes of the tyrosine environments and to assess their possible roles in the interface recognition site. These studies confirmed other physical studies that assigned Tyr-55 to a free, surface-exposed region of the molecule and Tyr-59 to a somewhat buried surface position in the protein tertiary structure. Chemical modification of Tyr-59 did not significantly decrease the coenzymatic activity of colipase, but in the case of Tyr-55, modification actually increased activity.

The earliest publication concerning the aminodansylation of Tyr-55 in porcine colipase [11] suggested, by comparison to conclusions from similar studies of PLA2 [12], that Tyr-55 was inserted into the interior of TDOC micelles as part of the micelle binding mechanism. This conclusion was based on a 70 nm blue shift and 4.3-fold quantum yield increase in the emission spectrum of DNS-Tyr-55 porcine colipase in the presence of levels of TDOC greater than the CMC. These considerable changes in emission properties are indicative of movement from a highly polar region to a very hydrophobic environment for DNS-Tyr-55. This paper presents time-resolved fluorescence studies of DNS-Tyr-55 porcine colipase to confirm the insertion of Tyr-55 into lipid interfaces.

Fluorescence lifetime analysis of the effect of TDOC micelle binding on DNS-Tyr-55 is in

agreement with static methods. Above CMC levels of TDOC the lifetime shifts from 11.5 to 15 ns, an increase which can be attributed to the movement of a fluorophore to a more hydrophobic environment. It is also worth noting that the lifetime of the model compound *N*-acetyl-3-aminodansyltyrosine ethyl ester is 13 ns in aqueous buffers and shifts to 15.2 ns in the highly viscous solvent propylene glycol [6]. The interior of the micelle would provide a considerably more viscous environment than the normal water solvent and may be one of the contributing factors in the increase in lifetime for DNS-Tyr-55 in the presence of TDOC. The second lifetime component of the emission decay of DNS-Tyr-55 porcine colipase is insensitive to micelle binding. The reason for the lack of any effect on the second component may be due to the geometry of specific rotameric isomers of dansyltyrosine that are unable or unlikely to interact with micelles [6]. Acrylamide quenching showed a decrease in accessibility of quencher for DNS-Tyr-55 when the modified protein was bound to a micelle. Again, these data can be explained by a model in which DNS-Tyr-55 is buried in the micelle when the colipase-micelle complex is formed; thus protecting it from quenching agents.

In order to use polarization and anisotropy decay data to study the effect of micelle binding on the local environment of DNS-Tyr-55 and DNS-Tyr-59, it was necessary to synthesize a derivative of colipase with a fluorophore in a region of the molecule that did not interact with bound micelles. This was accomplished by preferentially dansylating the N-terminus of colipase. Emission spectrum and lifetime analyses showed no changes with the addition of CMC levels of TDOC. By comparing polarization and anisotropy data of DNS-Gly-1 porcine colipase to DNS-Tyr-55 porcine colipase and DNS-Tyr-59 porcine colipase, it was possible to determine local changes by comparison. The polarization of DNS-Tyr-55 porcine colipase increased 100% from 0.0 to 12.5 mM TDOC while that of DNS-Gly-1 porcine colipase increased only 14%. This shows that local rotational changes at DNS-Tyr-55 are the cause of the additional increase in polarization. These changes may be due to hindered rotation of the fluorophore or decreased rotational rate or both. Anisotropy decay analysis utilizing the hindered fluorophore model showed that DNS-Tyr-55 is free to rotate until CMC levels of TDOC are reached. Increasing TDOC concentrations did not affect the r_{inf} value for DNS-Gly-1 porcine colipase. The limiting anisotropy at infinite time for DNS-Tyr-55 porcine colipase has a value of zero until 1.0 mM TDOC, at which it then increases to 0.028. This indicates that the angular displacement of the fluorophore is unable to complete its full rotation when the protein is bound to micelle. The rotational relaxation time of DNS-Tyr-55 porcine colipase increases 191% from 0.0 to 12.5 mM TDOC while the R value of DNS-Gly-1 porcine colipase increases 87% and of DNS-Tyr-59 porcine colipase 67% over the same range. By comparison this would indicate that the rotational time of the fluorophore is slowed by the presence of bound micelle. A model in which DNS-Tyr-55 is directly inserted into the interior of bound micelles would explain all the changes in emission, lifetime, quenching, polarization, and anisotropy decay observed when DNS-Tyr-55 porcine colipase binds TDOC micelles.

Micelle-colipase complex formation does not induce the same fluorescence changes when monitored by a probe at Tyr-59. The emission spectrum of DNS-Tyr-59 porcine colipase shows a 2-fold quantum yield increase in the presence of CMC levels of TDOC, but has no blue shift in emission maximum as in DNS-Tyr-55 porcine colipase. The first center of the lifetime distribution ($C[1]$) of DNS-Tyr-59 porcine colipase is not affected by TDOC concentration, in contrast with the first lifetime component of Tyr-55. Acrylamide quenching studies show that the dansyl group attached to Tyr-59 becomes more accessible to quencher when the protein is bound to micelle. This would suggest that a conformational change brought about by TDOC binding alters the protein structure in such a way as to move Tyr-59 to the surface of the molecule or perhaps opens the structure to allow solvent to be more accessible to Tyr-59. By comparing DNS-Tyr-59 porcine colipase, DNS-Tyr-55 porcine colipase and DNS-Gly-1 porcine colipase local changes in DNS-Tyr-59 polarization can be deduced. The polarization

of DNS-Tyr-59 porcine colipase does not change with added TDOC, while DNS-Gly-1 porcine colipase displays a 14% increase and DNS-Tyr-55 porcine colipase a 100% increase. The rotational relaxation time (R) of DNS-Gly-1 porcine colipase increases 83% and that of DNS-Tyr-55 porcine colipase 191% from 0.0 to 12.5 mM TDOC while R for DNS-Gly-1 only increases 67%. These data would suggest that Tyr-59 is not hindered when colipase is bound to a micelle. The fluorescence properties of DNS-Tyr-59 porcine colipase indicate that Tyr-59 does not interact with TDOC micelles in the direct manner in which Tyr-55 does, but may monitor a conformational change in the protein near its environment when colipase binds to a micelle, as shown by acrylamide quenching.

The increase in activity of DNS-Tyr-55 porcine colipase may be explained by the hydrophobic nature of the naphthalene ring of aminodansyltyrosine 55. Studies of the model compound *N*-acetyl-*o*-aminodansyltyrosine ethyl ester show that due to the hydrophobic nature of the aromatic rings, this molecule will preferentially partition into *n*-hexadecylphosphocholine micelles [12]. The hydrophobicity of the probe may increase the affinity of colipase for lipid interfaces. To examine this possibility, dissociation constants for TDOC micelle-colipase binding were calculated by Scatchard analysis of the titration of DNS-Tyr-55 porcine colipase with TDOC, as monitored by several different physical parameters. The published binding constant of colipase binding to bile salt micelles is 10^{-4} M [9,28]. The dissociation constants as determined by lifetime, polarization and anisotropy decay parameters all indicate that the Tyr-55 aminodansylated derivative of colipase has a higher affinity for the micelle than the unmodified protein. This might lead to the conclusion that a dansyl probe might direct itself towards lipid and as such be misleading as a probe for studying protein-lipid interactions.

The activity of the more polar nitrotyrosine 55 porcine colipase is not increased or diminished as compared to the native cofactor [33]. This suggests that the hydrophobic nature of the dansyl group is at least partially responsible for increased activity. However, dansylation at Tyr-59 and at the N-terminus does not stimulate activity nor does dansylation of Tyr residues in equine colipase (McIntyre, unpublished data). The model compound *N*-acetyl-*o*-aminodansyltyrosine ethyl ester does not show significant fluorescence changes in the presence of CMC levels of TDOC (McIntyre, unpublished data), suggesting that the dansyl group does not favor lipid environments in and of itself. The dansyl group at tyrosine may increase the activity of the colipase-lipase enzyme complex by increasing the affinity of colipase for interface. This would indicate that the dansyl group must be oriented in a position to be able to interact with lipid interfaces.

Chemical modification and spectrofluorometric studies of Tyr-55 and Tyr-59 presented in this paper indicate that Tyr-55 directly interacts with bound bile salt micelles. This interaction is best described as an insertion of the residue into the micelle interior. The importance of this residue in interface recognition and binding will now be further addressed by site-directed mutagenesis. Tyr-59 of porcine colipase does not interact with micelles as does Tyr-55, but may be located in a region of the molecule that is conformationally changed by colipase-micelle complex formation. The nature of the structural changes induced by micelle binding will be further investigated by the combined use of molecular genetics, biochemistry and biophysics.

Acknowledgements

This work was supported in part by NIH grants GM 31651 and DK 41402 to F.S.

References

1 L.G. Lange, III, J.F. Riordan and B.L. Vallee, Biochemistry 13 (1974) 4361.
2 W.D. Behnke and B.L. Vallee, Biochem. Biophys. Res. Commun. 43 (1971) 760.
3 R.A. Kenner and H. Neurath, Biochemistry 10 (1971) 551.
4 M.H. Caruthers, Protein engineering (A.R. Liss, New York, 1987) p. 65.
5a W.J. Rutter, S.J. Gardell, S. Roczniak, D. Hilvert, S. Sprnag, R.J. Fletterick and C.S. Craik, Protein engineering (A.R. Liss, New York, 1987) p. 257.

5b E.E. Howell, R.J. Mayer, M.S. Warren, J.E. Villafranca, J. Kraut and S.J. Benkovic, Protein engineering (A.R. Liss, New York, 1987) p. 251.
6 J.C. McIntyre, F. Schroeder and W.D. Behnke, Biochemistry 29 (1990) 2092.
7 T. Wieloch, B. Borgström, K.E. Falk and S. Forsen, Biochemistry 18 (1979) 1622.
8 J. Donner, C.H. Spink, B. Borgström and I. Sjoholm, Biochemistry 15 (1976) 5413.
9 H. Sari, B. Entressangles and P. Desnuelle, Eur. J. Biochem. 58 (1975) 561.
10 P.J. Cozzone, P. Canioni, L. Sarda and R. Kaptein, Eur. J. Biochem. 114 (1981) 119.
11 J.C. McIntyre, P. Hundley and W.D. Behnke, Biochem. J. 245 (1987) 821.
12 H. Meyer, W.C. Puijk, R. Dijkman, M.M.E.L. Foda-Vander Hoorn, F. Pattus, A.J. Slotboom and G.H. DeHaas, Biochemistry 18 (1979) 3589.
13a B.W. Dijkstra, K.H. Kalk, W.G.J. Hol and J. Drenth, J. Mol. Biol. 147 (1981) 97.
13b B.W. Dijkstra, J. Drenth and K.H. Kalk, Nature 289 (1981) 604.
14 C. Chapus, P. Desnuelle and E. Foglizzo, Eur. J. Biochem. 115 (1981) 99.
15 S. Granon, Biochim. Biophys. Acta 874 (1986) 54.
16 J.D. Johnson, J.H. Collins and J.D. Potter, J. Biol. Chem. 253 (1978) 6451.
17 G. Nemecz and F. Schroeder, Biochemistry 27 (1988) 7740.
18 W.D. Sweet, W.G. Wood and F. Schroeder, Biochemistry 26 (1987) 2828.
19 F. Schroeder, Y. Barenholz, E. Gratton, and T.E. Thompson, Biochemistry 26 (1987) 2441.
20 R.T. Fischer, M.D. Cowlen, M.E. Dempsey and F.S. Schroeder, Biochemistry 24 (1985) 3322.
21 J.R. Lakowicz, H. Cherek and A.J. Balter, Biochem. Biophys. Methods 5 (1981) 131.
22 J.R. Lakowicz, G. Laczko, H. Cherek, E. Gratton and M. Linkeman, Biophys. J. 46 (1984) 463.
23 R. Fiorini, M. Valentino, S. Wang, M. Glaser and E. Gratton, Biochemistry 26 (1987) 3864.
24 M.S. Caceri and W.P. Cacheris, Byte 9 (1980) 340.
25 J.R. Alcala, E. Gratton and F.G. Prendergast, Biophys. J. 51 (1987) 587.
26 J.R. Alcala, E. Gratton and F.G. Prendergast, Biophys. J. 51 (1987) 597.
27 M.R. Eftink and C.A. Ghiron, Biochemistry 23 (1984) 3891.
28 M. Charles, M. Astier, P. Sauve and P. Desnuelle, Eur. J. Biochem. 58 (1975) 555.
29 M. Charles, M. Séméniva and M. Chabre, J. Mol. Biol. 139 (1980) 297.
30 J.R. Lakowicz, Principles of fluorescence spectroscopy (Plenum, New York, 1983).
31 G. Scatchard, Ann. N.Y. Acad. Sci. 51 (1949) 660.
32 B. Borgström and H.L. Brockman, Lipases (Elsevier, New York, 1984).
33 J.D. DeCaro, W.D. Behnke, J.J. Bonicel, P.A. Desnuelle and M. Rovery, Biochim. Biophys. Acta 747 (1983) 253.